Selective Oxidation of Propylene to Propylene Oxide over Silver-Supported Tungsten Oxide Nanostructure with Molecular Oxygen

Shilpi Ghosh, Shankha S. Acharyya, Ritesh Tiwari, Bipul Sarkar, Rajib K. Singha, Chandrashekar Pendem, Takehiko Sasaki,[†] and Rajaram Bal*

Catalytic Conversion & Processes Division, CSIR-Indian Institute of Petroleum, Dehradun-248005, India

S *Supporting Information*

ABSTRACT: Propylene oxide (PO) is a versatile chemical intermediate, and by volume it is among the top 50 chemicals produced in the world. The catalytic conversion of propylene to PO by molecular oxygen with minimum waste production is of high significance from an academic as well as an industrial point of view. We have developed a new synthesis strategy to prepare 2−5 nm metallic silver nanoparticles (AgNPs) supported on tungsten oxide (WO_3) nanorods with diameters between 30 and 40 nm, in the presence of cationic surfactant (cetyltrimethylammonium bromide: CTAB), capping agent (polyvinylpyrrolidone: PVP), and hydrazine. The synergy between the surface AgNPs and WO_3 nanorods facilitates the dissociation of molecular oxygen on the metallic Ag surface to produce silver oxide, which then transfers its oxygen to the propylene to form PO selectively. The catalyst exhibits a PO production rate of 6.1×10^{-2} mol g_{cat}^{-1} h^{-1}, which is almost comparable with the industrial ethylene-to-ethylene oxide production rate.

KEYWORDS: *selective oxidation, propylene oxidation, propylene oxide, molecular oxygen, silver nanoparticles, tungsten oxide nanorod*
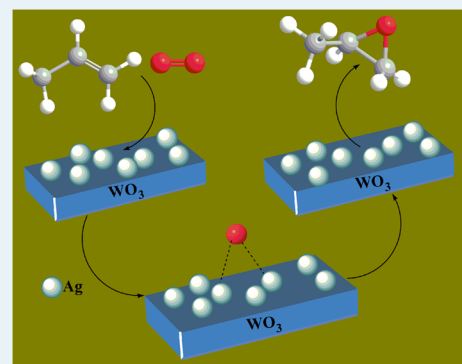
Propylene oxide (PO) is one of the most important synthetic intermediates produced in the industry to make various commodity chemicals, such as polyeurethane foams, propylene glycol, polypropylene glycol, propylene carbonate, etc., and currently, its production exceeds 10 million tons per annum.[1] Ninety percent of the world production of PO is produced either through a chlorohydrin process or by an organic hydroperoxide process (Halcon method).[2] Apart from acute environmental problems, the chlorohydrin process is also associated with equipment corrosion due to the usage of significant amount of chlorine. In addition, the Halcon process involves autoxidation of ethylbenzene or isobutene to produce alkylhydroperoxide, which finally acts as an oxidant to produce PO, accompanied by substantial formation of unwanted byproduct, peroxycarboxylate.[2] Thus, the selective oxidation of propylene to PO, in an economically viable and more environmentally friendly means, without producing minimal waste, is of paramount importance.

The selective oxidation of propylene to PO is regarded as the Holy Grail in catalysis.[3] The main difficulty arising for PO production is the presence of labile allylic H atom, which is more susceptible to combustion through C−H cleavage.[4] Haruta and co-workers reported selective oxidation of propylene to PO mediated by 2−4 nm gold nanoparticles on titania in the presence of O_2 and H_2.[5] Although the selectivity for PO is high, the use of H_2 suffers from its high cost and low efficiency, and the selectivity is greatly dependent on the size and morphology of the gold nanoparticles.[5,6] There is no reported catalyst to date that can be used industrially to produce propylene oxide directly from propylene using solely environmentally benign molecular oxygen.

It has been reported in the literature that supported Ag catalyst activates molecular oxygen, and the activity of the catalyst largely depends on the size of the Ag particles.[7] Although supported silver catalyst has been employed successfully for the epoxidation of ethylene to ethylene oxide on a commercial scale, successful implementation of silver in the propylene epoxidation reaction has not been reported so far because of either low conversion or poor PO selectivity.[8] Recently, Lei et al. reported that AgNPs supported on Al_2O_3 with a narrow particle size distribution is a prerequisite for high catalytic activity of this reaction.[9] Here, we have designed a new synthesis strategy to prepare metallic AgNPs supported on WO_3 nanorod. In recent years, significant efforts have been devoted to the controlled synthesis of nanostructured silver particles, but most of the preparation methods are energy-intensive, require substantial heat treatment, and produce larger particles.[10] Supported WO_3 catalysts have been shown to be catalytically active for selective oxidation of propylene to propylene oxide in a H_2O_2 medium.[11] Although there have been several reports of preparation of AgNPs, to date, the controlled synthesis of dispersed ultrasmall AgNPs (<5 nm) supported on WO_3 nanorods (Ag/WO_3) has not been reported.

Herein, we report the preparation of 2−5 nm AgNPs supported on WO_3 nanorods with diameters of ∼30−40 nm for selective conversion of propylene to propylene oxide using only molecular O_2. The Ag/WO_3 catalyst exhibits ∼16% propylene conversion with PO selectivity of 83% in a continuous flow process, where a PO production rate of 6.1×10^{-2} mol g_{cat}^{-1} h^{-1} was achieved in a steady state condition.

The Ag/WO_3 catalyst was prepared in aqueous medium in the presence of surfactant cetyltrimethylammonium bromide (CTAB), polyvinylpyrrolidone (PVP), and hydrazine, where tungstic acid and $AgNO_3$ were used as the W and Ag sources, respectively. It is a well established phenomena that Ag, W, and CTAB exist in the form of Ag^+, WO_4^{2-}, CTA^+ in aqueous alkaline solution (pH >7).[12] Therefore, a kind of cooperative self-assembly between the cationic part of the surfactant, CTAB, and anionic species can be formed via electrostatic interaction.[12] When the CTAB concentration become high (more than critical micelle concentration), cationic CTA^+ molecules start adsorbing onto the surface of the WO_4^{2-} ions and form spherical micelles.[13]

The curvature of an ionic micelle can be tuned from a spherical to a rodlike micelle by adding certain additives.[14] In our preparation method, the spherical micelles of CTAB−WO_4^{1-} were transformed into rod-shaped micelles as a result of attractive electrostatic interaction between the CTAB-stabilized negatively charged tungstate ions and the positively charged silver ions, where Ag^+ ions trigger symmetry-breaking anisotropic growth through selective adsorption onto particular crystal planes of tungsten. Thus, the decrease in surface energy of the WO_3 seed crystals in one direction results in the formation of a 1-D rodlike micellar structure, and this acts as the nucleating agent for the growth of the WO_3 nanorod. We observed that the amount of silver ions present in the solution has a pronounced influence on the nanorod growth.[15] Ag loading between 4 and 15 wt % leads to predominantly 1-D growth, and above 15 wt % Ag loading, different morphologies were observed (Figures 1, 2 and Supporting Information (SI)
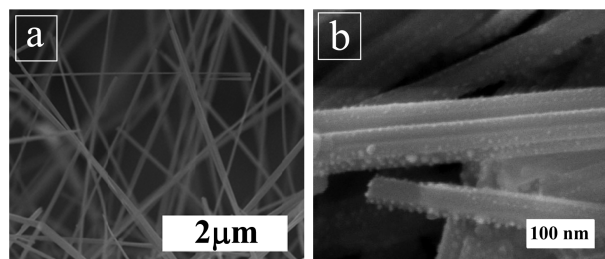

Figure 1. SEM images of fresh Ag/WO_3 catalyst (4.8 wt % Ag loading): (a) lower magnification, (b) higher magnification.

Figures S1, S2). It was found that PVP changes the size of the AgNPs rather than changing the size of the tungsten oxide nanorods. It was also observed that in the absence of PVP, Ag particles with nonuniform size (>5 nm) were formed (SI Figure S3). We believe that PVP coordinates easily with the Ag^+ surface with its carbonyl end and prevents aggregation of Ag particles. Generally, hydrazine reduces Ag^+ through formation of a complex Ag $(N_2H_4)^+$.[16] Being a reducing agent, hydrazine reduces Ag^+ to Ag onto the surface of WO_4^{2-}, thus discarding the formation of AgBr, and we observed only metallic silver deposition on the WO_3 surface. Thus, well-defined 2−5 nm AgNPs supported on WO_3 nanorods with diameters between
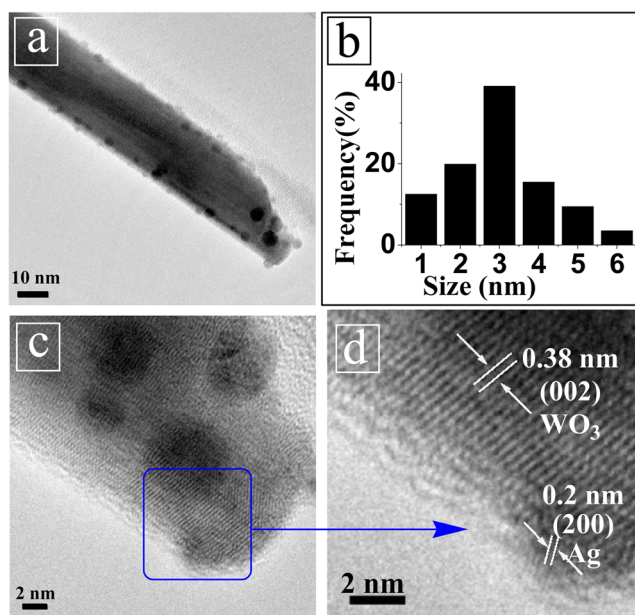

Figure 2. TEM images of (a) Ag/WO_3 catalyst (Ag loading 4.8 wt %), (b) AgNPs size distribution, (c) high-resolution image, and (d) lattice fringes.

30 and 40 nm can be prepared by mixing a particular amount of Ag, W, CTAB, hydrazine, and PVP. The rod-like morphology of WO_3 helps to increase the dispersion of metallic Ag, which ultimately facilitates easy access of oxygen to adsorb on it to form Ag_2O, which is the surface active oxygen species.[17]

Metallic AgNPs with size (2−5 nm) supported on WO_3 with diameter 30−40 nm can be imaged by SEM and TEM (Figures 1, 2). The lattice fringe with a *d*-spacing of 0.38 nm corresponds to the [020] plane of WO_3, and the distance of 0.20 nm corresponding to the [200] plane of Ag (Figure 2b) can also be seen. It should be noted that the pure WO_3 phase was formed without forming any substoichiometric WO_{3-x} phase. The W $4f_{5/2}$ and $4f_{7/2}$ spectra attributed to the binding energies 38.06 and 35.9 eV, respectively, suggest that the tungsten in the tungsten oxide nanostructure exists as W^{6+}.[18] The absence of a binding energy peak at 34.8 eV confirms that there is no substoichiometric WO_{3-x} present in the sample (SI Figure S4).[18] The X-ray diffraction peaks at 2θ values of 23.2°, 23.5°, 24.3°, 33.2°, and 34.2° depict the formation of WO_3 monoclinic structure (JCPDS No. 43-1035; space group, $P21/n$), and the peaks at 38.1° (111), 44.3° (200), 64.4° (220), and 77.4° (311) indicate the presence of metallic silver in the catalyst (JCPDS No. 04-0783) (Figure 3). The XPS spectrum of the fresh catalyst showed a Ag $3d_{5/2}$ binding energy value of 368.6 eV and a Ag $3d_{7/2}$ binding energy value of 374.6 eV (Figure 4). It is reported that the Ag 3d binding energy value changes with the particle size.[9,19] We can say that in our prepared Ag/WO_3 catalyst, because the Ag NPs are very small in size (2−5 nm), they exhibit a higher Ag 3d 5/2 binding energy value of 368.6 eV compared with the metallic Ag powder (368.2 eV) generally used as reference. Hence, we can say that the Ag 3d binding energy in our catalyst corresponds to metallic silver.

The metallic state of the Ag was also confirmed by EXAFS, in which the Ag−Ag bond length of 2.87 Å with a coordination number (C.N.) of 6.3 was observed (Supporting Information, Table S1, Figure S5a). The association of CTA^+ and PVP with
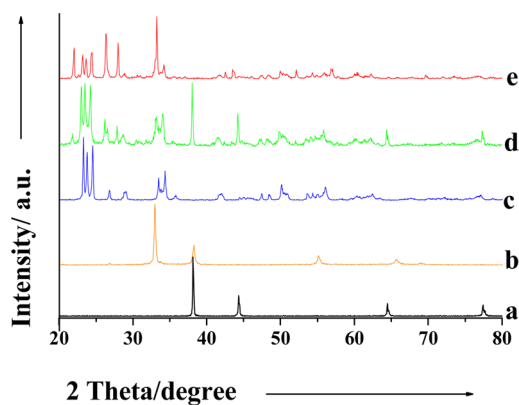
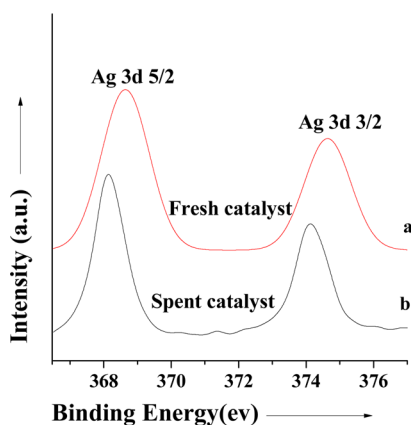**Figure 3.** XRD patterns of (a) Ag(0), (b) Ag(I) oxide, (c) W(VI) oxide, (d) fresh Ag/WO$_3$, and (e) spent Ag/WO$_3$.

Figure 4. Ag 3d core level spectra: (a) fresh Ag/WO$_3$ and (b) spent Ag/WO$_3$.

the WO$_4^{2-}$ and Ag$^+$ crystals were confirmed by TGA and FTIR analyses (Supporting Information, Figures S6, S7). The TGA curve depicts a decomposition peak around 400 °C, which is consistent with the decomposition temperature of CTAB. A total 13.9% mass loss suggests that surfactant molecules remain strongly associated with the WO$_4^{2-}$ and Ag$^+$ crystals for the as-synthesized sample. Moreover, the morphology is not affected by the removal of surfactant during calcination.

To get further support for the association of PVP and CTAB, FTIR was taken for the calcined and uncalcined samples. The FTIR spectra of the uncalcined sample exhibit the presence of C≡N, C=O, N$^+$−CH$_3$, and C−H functional groups. The peaks between 700 and 900 cm^{-1} can be assigned to bridging O−W−O.[20] The vibrational band at 1628 cm^{-1} may be assignable to C=O stretching, which is consistent with the presence of PVP.[21] A sharp, intense peak at 1408 cm^{-1} may be attributed to the C−N bond of the CTA$^+$ moiety.[22] Thus, the presence of C≡N, C=O, and N$^+$−CH$_3$ confirms that both CTAB and PVP is involved in the nanostructure growth process and control of the shape and size of the Ag nanoparticles and WO$_3$ nanorods.

The Ag/WO$_3$ nanostructure catalyst was studied for the propylene epoxidation reaction with molecular oxygen in a fixed-bed, high-pressure microreactor. The catalyst showed 15.5% propylene conversion with 83% selectivity toward propylene oxide at 250 °C and at 2 MPa pressure. It is a well-known phenomenon that the activation of molecular oxygen occurs by transferring charge density from metal to the

vacant π^* molecular orbital of adsorbed O$_2$.[23] In a silver-catalyzed system, high oxygen pressure would affect the activation energy for dissociative chemisorption of O$_2$ on the silver surface and accelerate the conversion of the silver surface to a silver oxide overlayer, as a result of which a loosely bonded Ag−O species is formed.[24] The XPS spectrum of our spent catalyst showed a Ag 3d$_{5/2}$ binding energy value of 368.2 eV, a negative binding energy shift of 0.4 eV from the fresh one (368.6 eV) (Figure 4b). It is known in the literature that the binding energy of Ag+ is lower than the metallic Ag and that the binding energy difference of the Ag 3d in a metallic and in an oxidized state is rather small.[9,25,26] As a continuation of the earlier reports, we can say that the binding energy shift of 0.4 eV for the spent catalyst (368.2 eV) indicates that metallic silver nanoparticles are partially oxidized after the reaction.[26,27]

The EXAFS analysis clearly indicates that after the reaction, silver is partially oxidized (SI Table S1, Figure S5b). The O 1s binding energy of the fresh catalyst exhibits a peak at 530.7 eV due to the W=O in WO$_3$,[18] and the O 1s spectrum of the spent catalyst showed two peaks, the peak at 530.8 eV and the additional small peak at 532.5 eV (Supporting Information Figures S8, S9). The binding energy value at 532.5 eV may be attributed to the oxygen species attached with Ag.[27] Ag K-edge extended X-ray absorption fine structure (EXAFS) analysis of the catalyst revealed significant changes in the silver species during the course of the propylene epoxidation reaction and showed that a Ag−O bond with a bond length of 2.349 Å is present in the spent catalyst (Supporting Information, Table S1, Figure S5b). This observation indicates that metallic Ag is being transformed to Ag$_2$O during the reaction.

We assume that the weakly associated Ag−O bond at 2.349 Å is the active oxygen species for propylene epoxidation reaction. We did a pulse experiment to check whether lattice oxygen is taking part during oxidation of propylene to propylene oxide transformation. When the pulse of propylene was used over the fresh Ag/WO$_3$ catalyst, no propylene oxide formation was detected. This clearly indicated that surface oxygen does not take part during the reaction. We then pretreated our catalyst with O$_2$ and measured the XPS of the catalyst and found Ag$_2$O was formed (from the binding energy shift of 0.3 eV, Supporting Information Figure S10). Then a propylene pulse was used over O$_2$ pretreated catalyst, and we noticed the formation of propylene oxide, so we conclude that during the reaction, metallic Ag was transformed to Ag$_2$O, which then converted propylene to propylene oxide. SI Figure S10 showed the Ag 3d XPS spectra after the O$_2$ treatment. XPS spectra were taken for the fresh catalyst after the pretreatment with O$_2$ and it was found that there is a negative binding energy shift (368.3 eV), as compared with the fresh catalyst (368.6 eV). In the fresh Ag/WO$_3$ catalyst, the highly intense band at 804 cm^{-1} in the Raman spectrum corresponds to the symmetric stretching vibration and the band at 708 cm^{-1} corresponds to the asymmetric stretching vibration of O−W−O bond, which coincides with bare WO$_3$ (Figure 5a, Figure 5b).[18] For the spent catalyst, the Raman spectrum (Figure 5c) showed a rather weak band around 524 cm^{-1}, which is attributed to Ag$_2$O species, owing to the Raman forbidden nature of Ag$_2$O, since oxygen atoms in silver oxide are located at inversion sites.[28] The intense peak at 936 cm^{-1} could be assigned to the γ (O=O) stretching mode of adsorbed molecular oxygen on silver,[23,28] and the peak at 367 cm^{-1} manifested due to δ (W−O−W) bending mode of bridging oxygens.[18] Thus, the
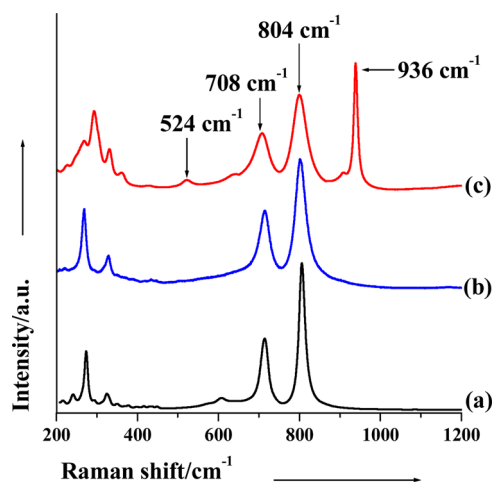
Figure 5. Raman spectra of (a) W (VI) Oxide, (b) fresh Ag/WO$_3$, and (c) spent Ag/WO$_3$.

Raman analysis is in full agreement with the EXAFS and XPS analysis.

The Ag/WO$_3$ nanostructure catalyst was inactive toward selective oxidation of propylene to propylene oxide with molecular oxygen at atmospheric pressure and a temperature below 150 °C, but the catalyst showed activity when both the pressure and temperature were increased. It is worth mentioning that PO is the dominant product during the reaction conditions over Ag/WO$_3$ (Ag loading was 4.8 wt %). Acrolein, acrylic acid, CO$_2$, and other oxygenated products were detected as side products (Table 1).

The effect of temperature was carried out with the Ag/WO$_3$ catalyst; the result is presented in SI Figure S11. It was observed that when the temperature is increased from 200 to 400 °C, conversion of propylene to PO increases from 9% to 27%, but a decreasing trend in PO selectivity (91% to 54%) was observed. The catalyst was inactive at a temperature below 150 °C. A PO selectivity of ~83% was observed after 6 h of reaction time at 250 °C using 4.8 wt % Ag loading catalyst. With increasing temperature, the selectivity to PO decreases, most probably because of the decomposition of propylene because we detected the formation of acetaldehyde, acetic acid, and formaldehyde as the main side products. A similar variation of propylene to PO conversion with different Ag loadings on the WO$_3$ surface was also observed (Table 1).

It was found that with increasing silver loading, although the conversion increases, the PO selectivity decreases. The catalyst with 4.8 wt % Ag loading exhibited a propylene conversion of 15.5% with 83% propylene oxide selectivity. The catalyst with

8.3% Ag loading showed a propylene conversion of 21% with 67% PO selectivity. The conversion increased to 26% with 58% PO selectivity when Ag loading was 14.6% (Table 1). We found that the higher Ag loading resulted in an increase in the average size of the AgNPs (15−20 nm with 8.3 wt % Ag loading, 30−50 nm with 14.6 wt % Ag loading) (Supporting Information, Figures S1, S2). It is very clear from the experiment that very small Ag NPs (<5 nm) facilitate the activation of molecular oxygen and selectively transform propylene to propylene oxide.

The effect of pressure is shown in SI Figure S12. We observed that pressure has a direct effect on the activation of molecular oxygen as well as the selectivity of PO. In a silver-catalyzed system, high oxygen pressure affects the activation energy for dissociative chemisorption of O$_2$ on the silver surface and accelerates the conversion of the silver surface to a silver oxide overlayer, as a result of which loosely bonded Ag−O species are formed.[24] The catalyst does not exhibit any activity at atmospheric pressure. At 1 MPa pressure, the conversion of propylene was ~7%, and the selectivity to PO was 39%, but with increasing pressure to 2 MPa, a significant increase in PO selectivity of 83% was observed. However, with additional pressure (3−4 MPa), although conversion increased, a significant lowering of the PO selectivity (55%) was observed as a result of the formation of carbon dioxide. This result is in conformity with that of silver-catalyzed ethylene epoxidation reaction, in which high oxygen pressure boosts the selectivity toward ethylene oxide.[24] We believe that Ag−O bond, with bond length of 2.349 Å that is slightly more than the normal Ag$_2$O (bond length 2.25 Å), could easily donate its labile oxygen atom to the C=C bond of propylene to form PO selectively. For this reason, our catalyst exhibited much better performance than that of other silver-catalyzed systems reported earlier (Supporting Information Table S2).

The effect of time on-stream is shown in SI Figure S13. It was observed that although the conversion was constant until 18 h, the PO selectivity decreases slightly after 18 h, from 83% to 79%. The plausible mechanistic pathway is shown in SI Scheme S1. We believe that initially, an oxygen molecule dissociates over the metallic Ag and a Ag$_2$O species with a Ag−O bond length of 2.349 Å is formed. This oxygen associated with Ag enables the formation of a four-membered cyclic transition state, with the propylene double bond followed by the insertion of oxygen into the C=C bond of propylene to form PO. This study is in conformity with the earlier report in which the direct abstraction of the O atom from Ag$_3$O to the double bond of propylene took place according to the Langmuir−Hinshelwood mechanism.[29]

Table 1. Catalytic Activities in Propylene Epoxidation Reaction[a]

entry	catalyst	loading of [Ag][b] (wt %)	propylene conversion[c] (%)	selectivity[d] (%)				PO production rate (mol POg$_{cat}$$^{-1}$ h^{-1})
				propylene oxide	acrolein	CO$_2$	other(s)[e]	
1[f]	Ag/WO$_3$	4.8	15.5	83	8	2	7	6.1 × 10^{-2}
2[g]	Ag/WO$_3$	8.3	21	67	13	5	15	3.7 × 10^{-2}
3[h]	Ag/WO$_3$	14.6	26	58	17	7	18	2.3 × 10^{-2}

[a]Reaction conditions: catalyst 0.30 g, reaction temperature = 250 °C, pressure = 2 MPa, feed gas C$_3$H$_6$ /O$_2$/Ar = 4/2/94, gas hourly space velocity (GHSV) = 16 000 mL g$_{cat}$$^{-1}$ h^{-1}, time on stream = 6 h. [b]Ag loadings estimated by inductively coupled plasma (ICP) atomic emission spectroscopy (AES) analysis. [c]Conversion of propylene = [moles of propylene reacted/initial moles of propylene used] × 100. [d]PO selectivity = (moles of PO formed/mol of propene converted) × 100. [e]Others include acrylic acid, acetic acid, acetaldehyde, and hydrocarbon. [f]Ag particles size 2−5 nm. [g]Ag particles size 15−20 nm. [h]Ag particles size 30−50 nm.

To find out whether isolated WO$_3$ nanorods are necessary for the propylene oxidation reaction, we prepared several other metal oxide supports and studied their catalytic activity (SI Table S3). The activities of the Ag catalyst supported on different group VI oxides, such as Cr$_2$O$_3$ and MoO$_3$, were found to be very low as compared with the Ag/WO$_3$ nanostructured catalysts. We also prepared CuO particles supported on WO$_3$ and found that the catalyst exhibits ~4% propylene conversion with 60% PO selectivity. Although the Cu catalyst showed good PO selectivity, the catalyst deactivation after 3 h may be due to the sintering of the Cu particles. Ag/WO$_3$ prepared by the conventional impregnation method showed irregular and larger particle sizes, leading to negligible (<5%) PO selectivity. Ag or WO$_3$ alone also does not exhibit any activity. The study revealed that using metallic AgNPs with 2−5 nm on WO$_3$ nanorods of 30−40 nm diameter is the key parameter for the catalytic activity, in which the rod-shaped tungsten oxide facilitates uniform dispersion of ultrasmall (<5 nm) AgNPs, which facilitates the dissociation of molecular oxygen to form Ag$_2$O. The synergistic effect between AgNPs and WO$_3$ nanorods plays the crucial role for the formation of PO, and the support tungsten oxide not only stops coalescence and agglomeration of the AgNPs but also highly supports PO formation. The Ag/WO$_3$ catalyst does not change its shape and size during propylene epoxidation reaction, as confirmed from TEM analysis (Supporting Information, Figure S14).

In summary, we explored an easy and facile synthesis strategy to prepare silver nanoparticles with size <5 nm supported on WO$_3$ nanorods with diameters of 30−40 nm using surfactant cetyltrimethylammonium bromide (CTAB), capping agent polyvinylpyrrolidone (PVP), and hydrazine. The metallic AgNPs supported on the WO$_3$ nanorods activated molecular oxygen, which can produce propylene oxide with very high selectivity directly from propylene without any additional reducing agent. The catalyst showed a propylene conversion of 15.5% with 83% PO selectivity at 250 °C using molecular oxygen. Using AgNPs of 2−5 nm and WO$_3$ nanorods with 30−40 nm diameters is the determining factor for propylene oxidation reaction. We believe that this promising catalyst may become a potential catalyst for other various oxidation reactions.

ASSOCIATED CONTENT

Ⓢ Supporting Information

Characterization techniques, experimental details, additional analysis data. This material is available free of charge via the Internet at http://pubs.acs.org.

AUTHOR INFORMATION

Corresponding Author
*E-mail: raja@iip.res.in.

Present Address
†(T.S.) Department of Complexity Science and Engineering, Graduate School of Frontier Sciences, The University of Tokyo, Kashiwanoha, Kashiwa-shi, Chiba 277−8561, Japan.

Notes
The authors declare no competing financial interest.

ACKNOWLEDGMENTS

REFERENCES

(1) (a) Cavani, F.; Teles, J. H. *ChemSusChem* **2009**, *2*, 508−534. (b) Nijhuis, T. A.; Musch, S.; Makkee, M.; Moulijn, J. A. *Appl. Catal., A* **2000**, *196*, 217−224.

(2) (a) Zuwei, X.; Ning, Z.; Yu, S.; Kunlan, L. *Science* **2001**, *292*, 1139−1141. (b) Nijhuis, T. A.; Makkee, M.; Moulijn, J. A.; Weckhuysen, B. M. *Ind. Eng. Chem. Res.* **2006**, *45*, 3447−3459. (c) Weissermel, K.; Arpe, H. J. *Industrial Organic Chemistry*, 4th ed.; Wiley-VCH: Weinheim, Germany, 2003, p 146.

(3) McCoy, M. *Chem. Eng. News* **2001**, *79*, 19−20.

(4) Vaughan, O. P. H.; Kyriakou, G.; Macleod, N.; Tikhov, M.; Lambert, R. M. *J. Catal.* **2005**, *236*, 401−404.

(5) Hayashi, T.; Tanaka, K.; Haruta, M. *J. Catal.* **1998**, *178*, 566−575.

(6) (a) Qi, C.; Okumura, M.; Akita, T.; Haruta, M. *Appl. Catal., A* **2004**, *263*, 19−26. (b) Haruta, M.; Date, M. *Appl. Catal.* **2001**, *222*, 427−437.

(7) (a) Qu, Z.; Cheng, M.; Huang, W.; Bao, X. *J. Catal.* **2005**, *229*, 446−458. (b) Van Santen, R. A.; Kuipers, H. P. C. E. *Adv. Catal.* **1987**, *35*, 265−321. (c) Lu, J.; Bravo-Suárez, J. J.; Atsushi Takahashi, A.; Haruta, M.; Oyama, S. T. *J. Catal.* **2005**, *232*, 85−95. (d) Molina, L. M.; Lee, S.; Sell, K.; Barcaro, G.; Fortunelli, A.; Lee, B.; Seifert, S.; Winans, R. E.; Elam, J. W.; Pellin, M. J.; Barke, I.; Oeynhausen, V. V.; Lei, Y.; Meyer, R. J.; Alonso, J. A.; Rodríguez, A. F.; Kleibert, A.; Giorgio, S.; Henry, C. R.; Meiwes-Broer, K. H.; Vajda, S. *Catal. Today* **2011**, *160*, 116−130.

(8) (a) Yao, W.; Guo, Y. L.; Liu, X. H.; Guo, Y.; Wang, Y. Q.; Wang, Y. S.; Zhang, Z. G.; Lu, G. Z. *Catal. Lett.* **2007**, *119*, 185−190. (b) Serafin, J. G.; Liu, A. C.; Seyedmonir, S. R. *J. Mol. Catal. A: Chem.* **1998**, *131*, 157−168. (c) Barteau, M. A.; Madix, R. J. *J. Am. Chem. Soc.* **1983**, *105*, 344−349. (d) Wang, R. P.; Guo, X. W.; Wang, X. S.; Hao, J. Q. *Catal. Today* **2004**, *93*−95, 217−222.

(9) Lei, Y.; Mehmood, F.; Lee, S.; Greeley, J.; Lee, B.; Seifert, S.; Winans, R. E.; Elam, J. W.; Meyer, R. J.; Redfern, P. C.; Teschner, D.; Schlögl, R.; Pellin, M. J.; Curtiss, L. A.; Vajda, S. *Science* **2010**, *328*, 224−228.

(10) (a) Li, Y.; Wu, Y.; Ong, B. S. *J. Am. Chem. Soc.* **2005**, *127*, 3266−3267. (b) Hiramatsu, H.; Osterloh, F. E. *Chem. Mater.* **2004**, *16*, 2509−2511. (c) Kashiwagi, Y.; Yamamoto, M.; Nakamoto, M. *J. Colloid Interface Sci.* **2006**, *300*, 169−175.

(11) Kamata, K.; Yonehara, K.; Sumida, Y.; Hirata, K.; Nojima, S.; Mizuno, N. *Angew. Chem., Int. Ed.* **2011**, *50*, 12062−12066.

(12) Zhou, Y. X.; Zhang, Q.; Gong, J. Y.; Yu, S. H. *J. Phys. Chem. C* **2008**, *112*, 13383−13389.

(13) De, S.; Mandal, S. *Colloids Surf., A* **2013**, *421*, 72−83.

(14) Lamont, R. E.; Ducker, W. A. *J. Am. Chem. Soc.* **1998**, *120*, 7602−7607.

(15) Jana, N. R. *Small* **2005**, *1*, 875−882.

(16) Tatarchuk, V. V.; Sergievskaya, A. P.; Korda, T. M.; Druzhinina, I. A.; Zaikovsky, V. I. *Chem. Mater.* **2013**, *25*, 3570−3579.

(17) Liang, X. L.; Dong, X.; Lin, G. D.; Zhang, H. B. *Appl. Catal., B* **2009**, *88*, 315−322.

(18) Breedon, M.; Spizzirri, P.; Taylor, M.; Plessis, J.; McCulloch, D.; Zhu, J.; Yu, L.; Hu, Z.; Rix, C.; Wlodarski, W.; Kalantar-zadeh, K. *Cryst. Growth Des.* **2010**, *10*, 430−439.

(19) Lim, D. C.; Lopez-Salido, I.; Kim, Y. D. *Surf. Sci.* **2005**, *598*, 96−103.

(20) Phuruangrat, A.; Ham, D. H.; Hong, S. J.; Thongtema, S.; Lee, J. S. *J. Mater. Chem.* **2010**, *20*, 1683−1690.

(21) Sun, H.; He, J.; Wang, J.; Zhang, S. Y.; Liu, C.; Sritharan, T.; Mhaisalkar, S.; Han, M. Y.; Wang, D.; Chen, H. *J. Am. Chem. Soc.* **2013**, *135*, 9099−9110.

(22) Sau, T. K.; Murphy, C. J. *Langmuir* **2005**, *21*, 2923−2929.

(23) Pulido, A.; Concepcion, P.; Boronat, M.; Corma, A. *J. Catal.* **2012**, *292*, 138−147.

(24) Van Santen, R. A.; Neurock, M. *Molecular Heterogeneous Catalysis: A Conceptual and Computational Approach*; Wiley-VCH: Weinheim, 2006; pp 39−40.

(25) Serezhkina, S. V.; Tyavlovskaya, E. A.; Shevchenko, G. P.; Rakhmanov, S. K. *J. Non-Cryst. Solids* **2005**, *351*, 35−40.

(26) Ferraria, A. M.; Carapeto, A. P.; Botelho do Rego, A. M. *Vaccum* **2012**, *86*, 1988−1991.

(27) Jeong, S. J.; Lim, D. C.; Boo, J. H.; Lee, S. B.; Hwang, H. N.; Hwang, C. C.; Kim, Y. D. *Appl. Catal., A* **2007**, *320*, 152−158.

(28) Pettinger, B.; Bao, X.; Wilcock, I.; Muhler, M.; Schlogl, R.; Ertl, G. *Angew. Chem., Int. Ed.* **1994**, *33*, 85−86.

(29) 53rd Annual Report on Research 2008 (46131-G5 by Randall Mayer).